ELECTROMAGNETIC CONTROL OF FLOW SEPARATION

Tom Weier, Gerd Mutschke, Uwe Fey, Vjatcheslav Avilov, Gunter Gerbeth

1. Introduction

The performance of fluid mechanical devices is often limited by flow separation. The form drag of cars, the efficiency of diffusers and the stall on airfoils are only some examples. Control of flow separation by suction was first demonstrated by Ludwig Prandtl [1] when he presented his boundary layer theory. Flow separation occurs when fluid decelerated by friction forces is exposed to an adverse pressure gradient which is stronger than the remaining kinetic energy of the fluid. Due to separation, form drag increases and possible lift decreases. To prevent separation, the momentum deficit of the boundary layer has to be overcome and the pressure gradient of the outer flow has to be balanced.

Numerous different techniques as, e.g. suction, blowing, and wall motion have been developed and many practical applications exist today e.g. in aerodynamics.
If the fluid is electrically conducting, an additional control possibility is given by the application of a Lorentz force **f**. This electromagnetic body force results from the vector product of the magnetic induction **B** and the current density **j**:

$$\boldsymbol{F} = \boldsymbol{j} \times \boldsymbol{B} \tag{1}$$

The current density is given by Ohm's law

$$\boldsymbol{J} = \sigma(\boldsymbol{E} + \boldsymbol{U} \times \boldsymbol{B}); \tag{2}$$

where **E** denotes the electric field, **U** the velocity and σ the electrical conductivity, respectively. Depending on the conductivity of the fluid, different control strategies exist. In case of low-conducting fluids as electrolytes or seawater ($\sigma \approx 10$ S/m), which will be considered in the following, induced currents $\sigma(\mathbf{U}\times\mathbf{B})$ alone are too small, and external electric fields have to be applied in order to control the flow. Therefore, also time-dependend forces might easily be established by supplying AC-voltage feeding of the electrodes. However, electrochemical aspects like the production of electrolytic bubbles have to be considered.

The following paper gives an overview about recent experimental results on separation control at inclined plates and airfoils. For that a simple geometry of alternating stripwise electrodes and magnets attached to the surface of the body (see Fig. 1) was used. This arrangement generates a surface-parallel Lorentz force which is exponentially decreasing in wall-normal direction. Singularities at the corners of the electrodes and magnets additionally cause a slight spanwise variation of the Lorentz force in regions very close to the surface (see Fig. 2). The exact force distribution, integrated over the spanwise coordinate *z*, is

$$F = \frac{\pi}{8} j_0 M_0 e^{-\frac{\pi}{a} y} \tag{3}$$

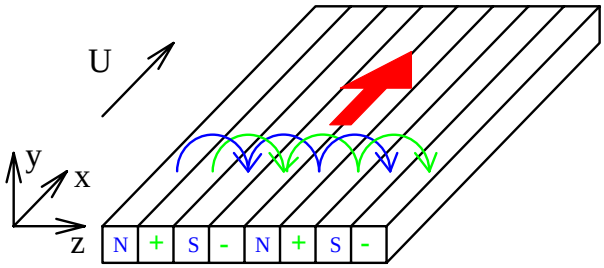

Fig.1: Sketch of the electric (green) and magnetic (blue) field lines and the resulting Lorentz force (red arrow) over a flat plate

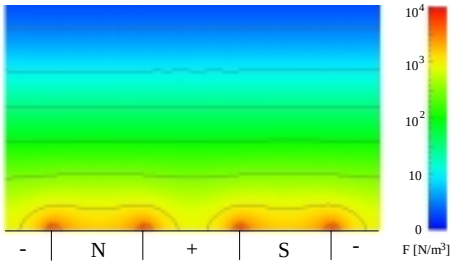

Fig. 2: Calculated Lorentz –force distribution

where M_0 denotes the magnetization of the magnets. Both electrodes and magnets are assumed to have the same width a.

The idea to influence the boundary layer flow of a low conducting fluid by electromagnetic forces dates back to the 1960s [2] and has recently attracted new attention for controlling turbulent boundary layers [3-6]. The first concept of Gailitis and Lielausis [2] used a streamwise Lorentz force for stabilizing a flat plate boundary layer. A tremendous reduction of skin friction will result from transition delay, since turbulent skin friction in general is orders of magnitude larger than laminar one. Following the approach of Tsinober and Shtern [8], the non-dimensional parameter

$$Z = \frac{1}{8\pi}\frac{j_0 M_0 a^2}{\rho U_0 \nu} \tag{4}$$

is obtained ("Tsinober-Shtern" parameter) by normalizing the boundary layer equations with the electromagnetic force term (3). Z describes the ratio of electromagnetic to viscous forces. ν, ρ and U_0 denote the kinematic viscosity, density and freestream velocity of the fluid, respectively. For the canonical case of a flat plate boundary layer, the streamwise pressure gradient dp/dx vanishes. Provided Z = 1, the boundary layer thickness reaches an asymptotic value. That means, the momentum loss due to the wall friction is just balanced by the momentum gain caused by the electromagnetic force. As consequence, an exponential boundary layer profile develops

$$\frac{u}{U_0} = 1 - e^{-\frac{\pi}{a}y} \tag{5}$$

comparable to the asymptotic suction profile. This profile has a critical Reynolds number which is two orders of magnitude higher than the one for the Blasius profile, i.e. transition will be delayed considerably.
The normalization of the Navier-Stokes equation leads to an additional non-dimensional parameter

$$N = \frac{j_0 B_0 L}{\rho U_0^2} \tag{6}$$

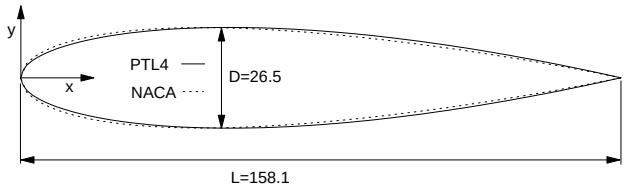

Fig.3: PTL-IV hydrofoil in comparison to a NACA-0017 airfoil

N is the so-called interaction parameter defining the ratio of electromagnetic to inertial forces. B_0 is the surface magnetization of the permanent magnets and *L* is a characteristic length. Obviously, *N* and *Z* are not independent, since $Z/N \sim Re$.

2. Experimental Apparatus

Flat plate boundary layer measurements and the investigation of the flow around a hydrofoil were carried out in a closed loop filled with the sodium chloride electrolyte at the Hamburg Ship Model Basin (HSVA). LDA measurements at the flat plate were performed on the upper plate side because of the electrolytic bubble production, but both sides of the plate were equipped with electrodes and magnets. The plate has 25 electrodes and 25 magnet strips, each 10 mm in width. The magnet/electrode array starts at 100 mm from the leading edge of the plate and has a length of 400 mm. The whole plate is 500mm×590mm in size and 18mm thick. Leading edge and trailing edge are rounded. The magnets generate an induction of 0.35T at their surface and consist of neodymium-iron-boron (NdFeB). The electrodes are made from stainless steel.
Separation prevention by electromagnetic forces has been studied on an additional small flat plate and two hydrofoils at different angles of attack.

The small flat plate is 130mm×140mm and 6mm thick. Electrodes and magnets cover the plate at 3mm from the leading edge and extend up to 37mm from the trailing edge. The width of the electrodes and magnets is a=10mm. Stainless steel has been used as electrode material in combination with a sodium hydroxide solution in the open channel. The permanent NdFeB magnets surface induction is B_0 = 0.4T. The hydrogen bubble technique has been applied to visualize the flow.

To verify the influence of separation prevention on the lift and the drag of a body, force measurements on two hydrofoils have been carried out at HSVA's Arctic Environmental Test Basin. Fig. 3 shows the geometry of the hydrofoil PTL-IV in comparison to a NACA 0017 airfoil. The hydrofoils with a span s of 360mm and additional end plates were mounted on a Kempf&Remmers force balance. All signals (drag, lift, angle of attack, pitching moment) were recorded by a standard PC.

The Arctic Environmental Test Basin is an open channel 30m long and 1.2m deep filled with the same aqueous sodium chloride. The maximum speed is about 1m/s. The two hydrofoils differ in their electromagnetic system. One has an electrode spacing of a = 5mm, the other of a=10mm. The magnets of the first hydrofoil have a surface induction of B_0 = 0.2T, those of the second one B_0 = 0.4T.

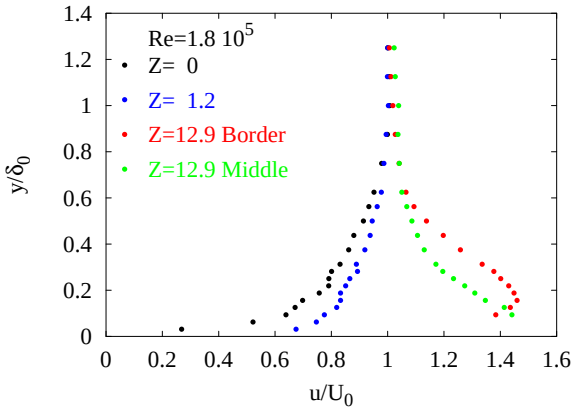

Fig. 4: Mean velocity profiles for the flat plate boundary layer in parallel flow

3. Results

3.1. Flat Plate

The effect of a streamwise Lorentz force on the mean velocity profile of a flat plate boundary layer is shown in Fig. 4. This profile was measured at the end of the electrode/magnet array, i.e. at x=500mm measured from the leading edge. A Reynolds number $Re=U_0x/\nu$ of $1.8\cdot10^5$ slightly below the theoretical transition value characterizes the flow. As can be seen from the fluctuating velocities without the Lorentz force (Z=0), the boundary layer flow is not laminar as it could be expected for such non-optimized conditions. A similar conclusion can be drawn by looking closer at the mean velocity profile. It is an intermediate profile between a Blasius and a logarithmic one. This early transition of the boundary layer is probably caused by the high turbulence level of 2% in the cavitation tunnel.

Thus the streamwise Lorentz force is, in contrast to the theory, applied to a turbulent boundary layer. For Z=1.2 the influence of the force on the flow consists in a moderate acceleration of the near wall fluid. The velocity profile becomes more convex near the wall, but ist shape is not an exponential one. Mainly three reasons could be responsible for this behavior. At first, the early transition of the boundary layer causes conditions not considered in the theory. Second, in order to establish the asymptotic profile, a certain evolution length has to be covered. A rough estimate can be given by looking at the definition of the dimensionless streamwise coordinate $x'=\nu\pi^2/(a^2U_0)$ which should at least be in the order of one to allow the asymptotic profile to develop. An integration of the boundary layer equations shows that at x'=7 the boundary layer profile for Z=1 has still a mean deviation of 1% from the exponential shape. The profiles in Fig. 4 are taken at x'= 0.13, i.e. at a position far from the required one. Third, the real force distribution differs from the ideal one. Their z modulations could have a destabilizing effect instead of the desired stabilizing one by possibly triggering transition due to secondary instabilities.

At a Tsinober-Shtern parameter of Z=12.9 the mean velocity profile shows the form of a wall jet, demonstrating the strong accelerating effect of the Lorentz-force. Fig. 4 gives the flow profile at two distinct positions in the spanwise coordinate z, at the border of a magnet and an

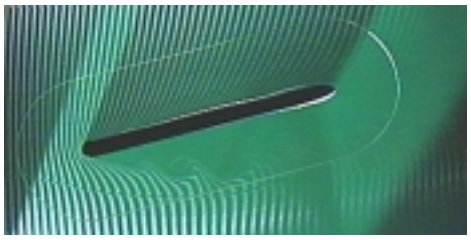

Fig. 5: Inclined plate: Lorentz force off

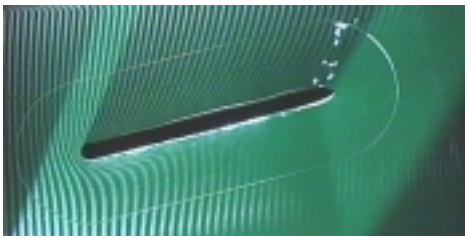

Fig. 6: Inclined plate: Lorentz force on

electrode and over the middle of a magnet. The result of the spanwise modulations on the velocity distribution is clearly to be seen. The flow is stronger accelerated at the force maxima, i.e. at the borders between electrodes and magnets (see Fig.2), than at the minima.

The wall jet in Fig.4 at Z=12.9 indicates the strong momentum increase in the boundary layer due to the Lorentz force. Since boundary layer separation occurs owing to an energy deficit of the near wall fluid, the streamwise Lorentz force should be able to counteract separation.

3.2. Inclined flat plate and hydrofoils

Visualizations of the flow around an inclined flat plate are given in Figs. 5 and 6. The electrolyte flows from the left to the right. Fig. 5 shows the flow around the plate without Lorentz force at an angle of attack $\alpha=15^{o}$. Since the Reynolds number based on the plate length is small ($Re=1.24\cdot10^{4}$), the flow separates laminar at the leading edge without reattachment. Because of the leading edge separation, the flow should be influenced already at the nose of the plate. Consequently the magnet/electrode-array is placed just behind the half cylinder forming the leading edge of the plate.

The flow situation under the influence of a Lorentz force of N=6.87 is shown in Fig. 6. As the bubble strips indicate, the boundary layer is attached over the whole length of the plate. Due to the pressure rise in the outer flow, the boundary layer fluid is strongly decelerated at the leading edge. By the Lorentz force, the near wall fluid is subjected to an acceleration while passing the plate. This can be seen by looking at the shape of the hydrogen bubble stripes near the plate.

Separation of flow causes a form or pressure drag on the moving body simply due to the pressure difference between forward and backward stagnation point. This form drag determines practically the total drag of bluff bodies at higher Reynolds numbers. Separation prevention can reduce the form drag to zero. The application of a streamwise Lorentz force for separation prevention has two additional consequences on the drag. On the one hand due to the exponential force distribution the velocity gradient at the wall and therefore wall friction is increased. On the other hand the force exerts thrust on the body. At high enough forcing parameters a configuration is possible, where thrust overcomes drag.

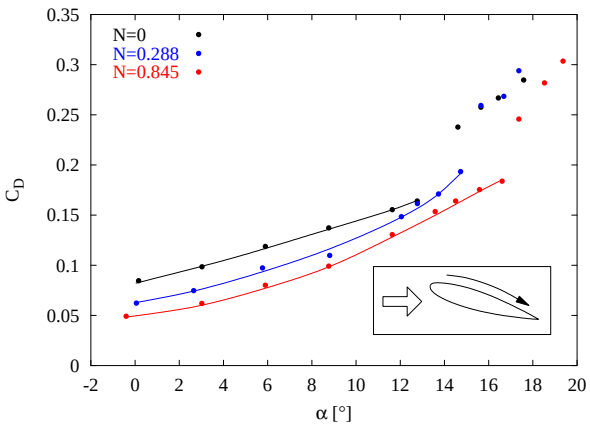

Fig. 7: C_D versus α for Re=4·10^4, a/L=0.03
and different interaction parameter

In Fig. 7 drag values of the PTL-IV hydrofoil with a/L=0.03 are presented for a Reynolds number Re=4·10^4 and different values of N versus the angle of attack α. The drag coefficient is defined in the usual way as

$$C_D = \frac{F_D}{\frac{\rho}{2} U_0^2 A} \tag{7}$$

with F_D denoting the total force in streamwise direction as obtained directly from the force balance measurements and A giving the wing area. The Lorentz force in Fig. 7 acts on the suction side of the hydrofoil only. At the low Reynolds number considered here, separation occurs for N=0 like at the flat plate as leading edge separation but at an higher inclination angle of 13°. Since the separation occurs abruptly a sudden increase of the drag coefficient is obtained. The application of the Lorentz force at the suction side results at small angles of attack, i.e. in a situation without separation, in a decrease of the drag coefficient due to the momentum gain caused by the force. The drag reduction is relatively moderate (ΔC_D=0.024 at N=0.288 and ΔC_D=0.037 at N=0.845). A larger effect on the drag results from the separation delay. At N=0.288 separation is delayed to α=14.7°, thereby reducing drag by ΔC_D=0.044. At N=0.845 separation occurs first at α=16.6°, resulting in a ΔC_D=0.084. The actual drag values are always compared to the values of the natural flow at the same angle of attack.

Thinking about drag reduction implies, of course, the question about the overall energetical balance. The small conductivity of typical electrolytes leads to large losses caused by Joule heating. It is clear that the drag reduction should overcompensate at least these Joule losses. Some hopes and estimates still exist for that based on the stabilization of a laminar boundary layer [2]; but to the best of the authors knowledge, no energetically efficient electromagnetic drag reduction has been demonstrated up to now.

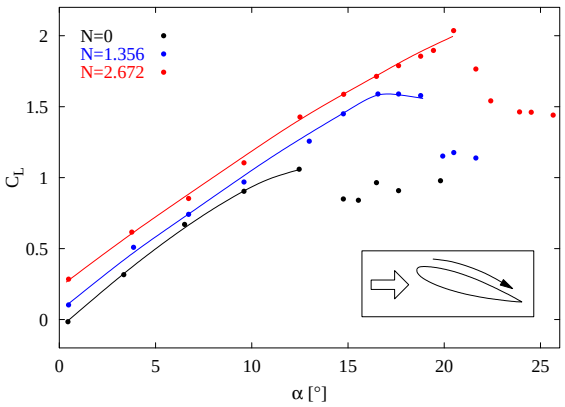

Fig. 8: C_L versus α for Re=2.9·10^4, a/L=0.06 and different interaction parameter

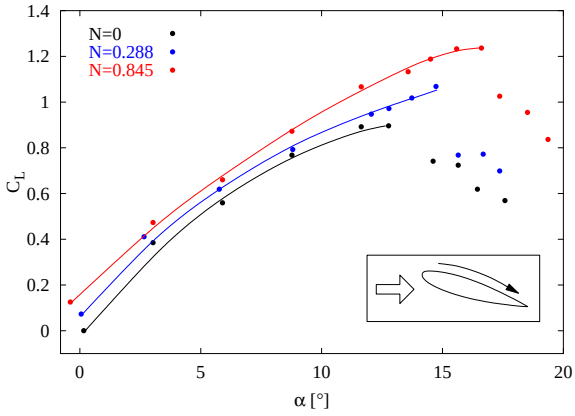

Fig. 9: C_L versus α for Re=4·10^4, a/L=0.03 and different interaction parameter

Especially on a hydrofoil, separation doesn't influence the drag alone, but also the lift. Figs. 8 and 9 show the lift development with the angle of attack at different N for the two hydrofoils. The lift coefficient is defined in analogy to the drag coefficient as

$$C_L = \frac{F_L}{\frac{\rho}{2} U_0^2 A} \tag{8}$$

Here F_L denotes the force on the hydrofoil in the direction normal to the liquid flow. Fig. 8 gives experimental values obtained at Re=2.9·10^4 and a/L=0.06, Fig. 10 for Re=4·10^4 and a/L=0.03. As in Fig. 7, the Lorentz force is applied at the suction side only. At N=0 separation takes place at α=13^o leading to an abrupt lift decrease. If the Lorentz force is switched on, already at small angles of attack a lift increase can be seen. This lift increase results from the additional circulation caused by the acceleration of the suction side flow. Corresponding to the drag reduction at small angles of attack, also the lift increase due to enhanced circulation is of moderate size. Nevertheless it is possible to obtain a lift force even without an inclination of the hydrofoil.

A much larger lift increase results from the delayed separation of the suction side flow at high angles of attack. The lift coefficient increases further monotonically with the angle of attack up to a point, where the Lorentz-force cannot any longer withstand the pressure gradient of the outer flow. From Fig. 8 one can detect, that for the hydrofoil with a/L=0.06 at Re =2.9·10^4 and N=2.67 stall can be delayed up to α=21^o. This results in an increase of the lift coefficient by 92% in comparison to the unforced flow. The same scenario is shown in Fig. 9 but for the hydrofoil with a/L=0.03 at Re =4·10^4 and N=0.84. Due to the lower interaction parameter, the hydrofoil stalls at α=17^o, the maximum lift increases by 43%.

4. Conclusions

Experimental demonstration of separation prevention on a circular cylinder by means of a streamwise Lorentz force with accompanying numerical simulations have been given in [9].

The influence of a streamwise Lorentz force on the flow along a flat plate has been studied in a saltwater flow. The experiments show a strong acceleration of the near wall flow if electromagnetic forces of sufficient strength are applied. The application of the streamwise force to the control of separation at an inclined plate and two hydrofoils has been successfully demonstrated. Stall is delayed to higher angles of attack resulting in an increase of maximum lift and a decrease of total drag of the hydrofoils.

Acknowledgments

Financial support from VDI under Grant NLD-FKZ 13N7134/1 is gratefully acknowledged. We would also like to thank the measuring crew from HSVA and Prof. Lielausis from IoP Riga for preparing a plate and an airfoil.

References

[1] L. Prandtl (1904), Über Flüssigkeitsbewegung bei sehr kleiner Reibung, Verhandlg. III. Intern. Math. Kongr. (pp.484-491), Heidelberg

[2] A. Gailitis and O. Lielausis (1961), On a possibility to reduce the hydrodynamical resistance of a plate in an electrolyte, Applied Magnetohydrodynamics. Reports of the Physics Institute 12 (pp. 143-146), Riga (in Russian)

[3] C. Henoch and J. Stace (1995), Experimental investigation of a salt water turbulent boundary layer modified by an applied streamwise magnetohydrodynamic body force, Phys. Fluids, 7, 1371

[4] C.H. Crawford and G.E. Karniadakis (1997), Reynolds stress analysis of EMHD-controlled wall turbulence. Part I. Streamwise forcing, Phys. Fluids, 9, 788

[5] J.C.S. Meng (1994), Seawater Electromagnetics: A new Frontier, Magnetohydrodynamics, 30, 401

[6] D.M. Nosenchuck and G. Brown (1993), Discrete spatial control of wall shear stress in a turbulent boundary layer, in R.M.C. So, C.G. Speziale and B.E. Launder (Ed.), Near-Wall Turbulent Flows (pp.689-698), Elsevier

[7] E. Grienberg (1961), On determination of properties of some potential fields, Applied Magnetohydrodynamics. Reports of the Physics Institute 12 (pp. 147-154), Riga (in Russian)

[8] A.B. Tsinober and A.G. Shtern (1967), On the possibility to increase the stability of the flow in the boundary layer by means of crossed electric and magnetic fields, Magnitnaya Gidrodinamica, 152

[9] T. Weier, G. Gerbeth, G. Mutschke, E. Platacis, O. Lielausis (1998), Experiments on cylinder wake stabilization in an electrolyte solution by means of electromagnetic forces localized on the cylinder surface. Experimental Thermal and Fluid Science, 16, 84